Macromolecules
ARTICLE

Macromolecules **2009**, *42*, 6231–6238 **6231**
DOI: 10.1021/ma901091j

Electrophoretic Mobility of Gold Nanoparticles in Thermoresponsive Hydrogels

A. Grimm, C. Nowak, J. Hoffmann, and W. Schartl*

Institut fur Physikalische Chemie, Welderweg 11, 55099 Mainz, Germany

Received May 19, 2009; Revised Manuscript Received June 29, 2009

ABSTRACT: We study the electrophoretic mobility of gold nanoparticles embedded in thermoresponsive poly(*N*-isopropylacrylamide) (PNIPAM) hydrogels by phase analysis dynamic light scattering (PALS). Approaching the phase transition temperature, the mobility of the nanoparticles strongly increases, which is related to a proceeding spinodal decomposition of the gel into polymer-poor regions and highly cross-linked polymer-rich domains, opening up larger pores which allow for enhanced migration of the embedded tracer particles. This effect, which is also relevant for thermally controlled release of nanoscopic substrates from thermoresponsive hydrogels, is explored in dependence of sample temperature, size of the gold nanoparticles, and structure of the hydrogel (polymer content and cross-linker content).

Introduction

The mobility of colloidal nanoparticles in a polymer gel matrix is mainly determined by the size of the particle with respect to the mesh size of the gel: for particles much smaller than the gel mesh size, the particle mobility should be identical to that found in a pure solvent. In case the particle size and mesh size are comparable, a much lower mobility of the tracer particles is expected. Finally, in case the particles are larger than the gel meshes, they should be completely immobilized. Although the movement of nanoscopic particles within gels, especially responsive gels so the particle speed can be manipulated by external stimuli as heat or light, is a very important issue relevant, for instance, in chromatography, drug delivery, etc.; so far only few studies on particle motion inside chemically cross-linked gels have been published.[1−8]

One major difficulty is the preparation of a well-defined homogeneous network as well as the characterization of the average mesh size and mesh size distribution. Usually, the gel is obtained from polymerization of a mixture of two different types of building blocks: a chain-forming monomer and a multifunctional cross-linker. The resulting gel structure depends on reaction temperature and concentrations of monomer and cross-linker, respectively.[9−12] For small monomer concentrations (<2 vol %) a heterogeneous gel is formed, consisting of tightly and loosely cross-linked regions. This may explain why even larger colloidal particles (size >100 nm) have been found to diffuse in such type of gels.[2]

Another important point is the actual meaning of the correlation length measured by dynamic light scattering from polymer gels, which often is interpreted as the mesh size of the system.[1] Shibayama et al. explored the tracer diffusion of polystyrene latex beads of size 85 nm within PNIPAM solutions and chemically cross-linked PNIPAM hydrogels by dynamic light scattering at room temperature.[8] They found that the mobility of their tracers became totally frozen at cross-linker concentrations larger than 1.25 mM and NIPAM concentration 0.2 M, corresponding to a cross-link ratio of 1:160. Interestingly, the correlation length of the hydrogel itself only varied from 5.9 nm without cross-linker to 7.6 nm at cross-linker concentration 8 mM, which is much smaller than the size of the tracer particles in all cases. Therefore, Shibayama et al. concluded that the ratio tracer size to gel correlation length is not an essential parameter governing the dynamics of probe diffusion, but the most significant factor is whether the system has a permanent infinite network of solid-like chemically cross-linked domains. It finally should be noted that according to extensive dynamic light scattering studies of chemically cross-linked gels these systems in many cases show nonergodic behavior:[13,14] relaxation times extracted from time-averaged intensity autocorrelation functions sometimes vary a lot with sample position (or scattering volume), and the intercept of the normalized amplitude time correlation function is well below the theoretical value of 1, effects which both are clear indications of structural heterogeneities on length scales larger than several hundred nanometers.

Besides the problem of nonhomogeneity and the resulting nonergodicity, an important reason why there exist only few laser light scattering studies of tracer diffusion within polymer gels is the problem of optical contrast. Here, the method of enhanced Raleigh scattering[15] provides a solution, as already shown in our previous dynamic light scattering studies where we used gold-doped and therefore light-absorbing silicon nanoparticles as optical tracers.[16,17] If laser light of wavelength close to the absorption band is used for the scattering experiment, the scattering contrast of the light-absorbing particles is strongly enhanced due to divergence of their refractive index. Under certain conditions, however, the light absorption of the colloidal particles may lead to unwanted side effects caused by local heating of the sample, like for example thermal convection.

As an interesting gel matrix, thermoresponsive PNIPAM hydrogels have attracted a lot of interest also in the context of controlled release systems, since this polymer undergoes a phase transition from soluble to insoluble at $T = 34-36$ °C close to the human body temperature.[10] If light-absorbing gold nanoparticles are embedded inside such a thermoresponsive hydrogel, the gel structure can be manipulated locally by light absorption and corresponding heating, as has been demonstrated in the pioneering work by Sershen et al.[18−20] and more recently by Shiotani et al.[21] The latter used strong IR laser light of power >490 mW to shrink a hydrogel sample filled with nanoscopic gold rods and thereby release small encapsulated dye molecules.

*Corresponding author. E-mail: schaertl@uni-mainz.de.

Published on Web 07/10/2009

Shibayama et al. have explored in detail by small-angle neutron scattering the change in gel structure with increasing temperature at constant pressure (isobar) and constant volume (isochore), showing that the hydrogel shows a spinodal decomposition into solution-like polymer-poor domains and a solid-like highly cross-linked polymer-rich phase.[22] The characteristic length scale of the solution-like domains increases with temperature and finally diverges at the transition temperature T = 34 °C, as also confirmed by Tokita and Tanaka, who describe the increase of the correlation length with increasing temperature in PNIPAM hydrogels as reversible increase of gel−solvent friction.[23] As shown by Shibayama et al. by dynamic light scattering measurements, this increase in average mesh size is more pronounced for the isochore gel than for the isobar gel.[22]

To our knowledge, no one has yet explored the interesting bicontinuous structure of PNIPAM gels at the phase transition by studying the mobility of nanoscopic tracer particles embedded in a PNIPAM hydrogel as a function of temperature, thereby also verifying independently the SANS results obtained by Shibayama and co-workers. This is the main goal of the present paper, where we study the electrophoretic mobility of nanoscopic gold tracer particles within thermoresponsive poly(*N*-isopropylacrylamide) (PNIPAM) hydrogels by phase analysis light scattering (PALS) as a function of sample temperature, gel composition, and nanoparticle size. Compared to conventional DLS, the PALS method has the big advantage that the directed electrophoretic mobility of the charged nanoscopic probe particles can easily be separated from the diffusional dynamics of the hydrogel matrix.

Experimental Section

Gold Nanoparticles. Spherical gold nanoparticles with diameters 20, 50, and 100 nm were bought from the company Plano GmbH, Wetzlar, Germany. The particle sizes provided by the manufacturer were confirmed independently by dynamic light scattering. These particles are negatively charged due to citrate groups at the particle surface.

Hydrogels. Typically, 0.78 g of the monomer *N*-isopropylacrylamide (NIPAM, M = 113 g/mol) (7 mmol), 2 mg of the cross-linker *N,N′*-methylenebis(acrylamide) (BIS, M = 154 g/mol) (0.013 mmol, corresponding to a cross-linker:monomer ratio of 1:550) and 8.6 mg of the photosensitizer and radical former ammonium persulfate (APS) were dissolved in 14 mL of water. 5 mL of the aqueous dispersion of citrate-stabilized gold particles and 24 μL of tetramethylethylendiamine (TEMED) were added, and part of this mixture was photopolymerized at room temperature within Malvern Zetasizer Nano-suited single-use capillary cuvettes DTS 1060 (Malvern) made from poly(ether−ether−ketone) (PEEK) and equipped with a palladium electrode (sample volume = 0.75 mL) for at least 1 h, using a 200 W Hg/Xe high-pressure lamp (Amko Co., Germany) for irradiation. To determine the mesh size or, better, correlation length, corresponding hydrogels without added gold were polymerized at room temperature within a 1 cm diameter cylindrical Suprasil light scattering cuvette (see below). All ingredients were filtered prior to photopolymerization to remove dust from the sample. During our studies, the polymer content and the NIPAM monomer to cross-linker ratio, and therefore the mesh structure of the hydrogels, were varied systematically (see Results and Discussion). Importantly, our gels showed no macroscopic shrinkage with increasing temperature, so they seem to be pinned by the walls of the sample cell. Therefore, the volume phase transition in our case is expected to follow more the isochore case than the isobare case both discussed by Shibayama et al.[22] This is in agreement with the fact that after annealing for 30 min the measured gold particle mobilities remained unchanged, so the phase transition in our samples occurs quite fast compared to the isobare case.

Dynamic Light Scattering. Our setup consisted of a Stabilite 2060-45 Ar^+ laser (Spectra-Physics), operating at a wavelength λ = 514 nm, as light source, an ALV Sp-125 goniometer to adjust the scattering angle, and a fiber-optic detector to measure the scattered intensity as a function of time. A commercial two-lens setup (ALV) was used to reduce the natural width of the laser beam to a diameter of less than 1 mm. Intensity−time correlation functions were obtained from the homodyne detected scattered intensity using an ALV 5000 hardware correlator and used to verify the size of our commercial gold nanoparticles in very dilute aqueous solution. These measurements were performed at three different low laser powers < 50 mW to exclude unwanted side effects caused by light absorption of the gold nanoparticles and local sample heating. Importantly, according to our previous studies such effects, especially thermal convection, play only a minor role in aqueous solution but become very important in organic solvents which have a much higher thermal expansion coefficient than water.

We determined the average mesh size or correlation length of our hydrogels by dynamic light scattering following Park and Johnson,[1] using the relation

$$D_{c,\mathrm{eff}} = \frac{D_c}{1-\varphi} = \frac{kT}{6\pi\eta\xi} \tag{1}$$

D_c is the (collective) diffusion coefficient extracted from the time−intensity correlation function of the DLS measurement and φ the polymer volume fraction of the gel.

The data acquisition time for all dynamic light scattering measurements was 60 s per correlation function. All samples were purified from dust by filtration with Millipore filters, pore size 0.45 μm, and put into cylindrical Suprasil light scattering cuvettes of diameter 10 mm. Gel samples without added gold nanoparticles where filtered before polymerization and then polymerized within the light scattering cuvette. During the measurement, the samples were placed in a toluene bath of adjustable temperature to avoid diffraction from the glass walls of the cuvette and to keep the average sample temperature constant.

Electrophoretic Mobility Measurements. *A. Theoretical Background.* Charged particles exposed to a constant electric field migrate with constant velocity in case electrostatic force and hydrodynamic friction cancel each other. The resulting electrophoretic mobility, which is the velocity normalized by the electric field strength, is given as

$$U_E = \frac{ze}{6\pi R_H \eta} \tag{2}$$

z is the number of elementary charges per particle, R_H the hydrodynamic radius of the particle, and η the viscosity of the solvent.

We can also express the electrophoretic mobility in dependence of the so-called zeta potential ζ of the moving particle and the dielectric constant ε of the solvent:[24]

$$U_E = \frac{2\varepsilon\zeta f(\kappa a)}{3\eta} \tag{3}$$

The so-called Henry function $f(\kappa a)$ depends on the size ratio of the dielectric double layer κ^{-1} to particle radius a and assumes a value of 1.5 for aqueous solutions within the Smoluchowski approximation.

B. Phase Analysis Light Scattering. Phase analysis light scattering (PALS) is a technical improvement of laser Doppler elektrophoresis (LDE), which combines dynamic light scattering and electrophoresis to measure the electrophoretic mobility of charged particles.[25] For small mobilities the Doppler effect and the corresponding frequency shift of the incident laser light beam become too small with respect to the reference light beam

for sufficient resolution of the interference pattern detected in standard LDE measurements. This problem is solved by the PALS technique, which is the working principle of the commercially available Malvern Zetasizer Nano. Here, the phase shift $\Phi_s(t)$ caused by the Doppler effect is detected. The time derivative of this phase shift provides a quantitative measurement of the particle velocity according to

$$\frac{d\Phi_s(t)}{dt} = \omega_s = q(v_e \pm v_c) = q[U_e E(t) \pm v_c] \quad (4)$$

ω_s is the Doppler frequency shift, q the scattering vector (or inverse length scale) of the experiment, v_e the electrophoretic velocity, and v_c the so-called field-induced collective velocity.

The Malvern Zetasizer uses a helium−neon laser with wavelength 633 nm as light source and is equipped with a thermostat to adjust the sample temperature during the measurement in the regime 2−90 °C. Our sample cells were single-use capillary cuvettes DTS 1060 (Malvern) made from poly(ether−ether−ketone) (PEEK) and equipped with a palladium electrode (see above).

The software of the Malvern Zetasizer determines the zeta potential and thereby the electrophoretic mobility (see eq 3) of the migrating nanoparticles, using the viscosity and the dielectric constant of the solvent water at given sample temperature as input parameters. If the zeta potential is assumed to be constant within the temperature range regarded here, the electrophoretic mobility still depends on temperature because of the temperature-dependent solvent properties as viscosity and dielectric constant. To eliminate these contributions, we normalized our data with the mobilities of the respective gold nanoparticles measured in pure water. Each PALS measurement is an average of 60 single measurements, leading to a statistic error of less than 10%. Importantly, in contrast to pure DLS, which is based on scattering contrast only, PALS allows to distinguish the unidirectional mobility of the charged gold particles from random diffusional relaxation processes of the uncharged gel matrix itself.

Results and Discussion

1. Sample Characterization. *Gold Nanoparticles*. The commercial gold nanoparticles (Plano) were characterized by DLS, independently confirming the size given by the commercial provider. We used spherical gold nanoparticles with diameters 20, 50, and 100 nm.

Hydrogels and Hydrogel−Gold Composites. Tables 1 and 2 summarize the composition and characteristics of hydrogel and hydrogel gold samples considered in this work. Besides sample composition, also the correlation length as determined by DLS at $T = 20$ °C is given. This correlation length in all cases was obtained for pure hydrogels without added gold nanoparticles, since the nonambiguous DLS characterization of the gel in the presence of strongly scattering gold tracers would have been more difficult. The results, however, should also be valid for hydrogel gold composite samples with comparable hydrogel composition, since in dynamic light scattering studies of hydrogel gold samples (shown elsewhere) we found no effect of a small amount of added gold nanoparticles on the dynamics of the PNIPAM hydrogel. In addition, the UV/vis spectra of aqueous pure gold solutions and PNIPAM hydrogels with embedded gold nanoparticles always looked identical, showing that the gold particles did not aggregate in the presence of the polymer during the polymerization reaction. Therefore, we concluded that the presence of a small amount of gold nanoparticles during photopolymerization does neither change the structure of the hydrogel nor lead to an aggregation of the gold particles due to, for example, depletion interactions. Also, we do not expect strong attractive interactions between polymer and gold particles; otherwise, the mobility of the particles should be much smaller than detected in our electrophoretic mobility measurements, where at higher sample temperature our smallest tracers nearly reach the mobility found in pure water as discussed below. The samples listed in Table 2 are arranged in a way to emphasize our systematic parameter variation, namely gold particle size, polymer concentration, and cross-linker amount.

Figure 1A shows a typical DLS amplitude time-correlation $g_1(q,\tau)$ for a pure PNIPAM hydrogel. The data could be fitted surprisingly well to a single-exponential decay to yield a diffusion coefficient and a correlation length or average mesh size according to eq 1, but for more accurate fitting a double-exponential decay had to be used, taking into account the slow mode visible in the figure. Importantly, all "mesh sizes" provided in Tables 1 and 2 were independent of scattering angle and sample position within an experimental error of ±1.5 nm, showing that the fast relaxation mode shows a q^2 scaling as expected (see Figure 1B) and that most of our gels behave fairly ergodic, that is, are homogeneous in mesh structure. It also should be noted that the intercept of the amplitude correlation function is nearly 1.0, an additional strong indication for the near-absence of dynamical heterogeneities. Another argument for the homogeneous structure of our hydrogels is their high optical

Table 1. Pure PNIPAM Hydrogel Samples: Composition and Correlation Length As Determined by DLS at $T = 20$ °C

hydrogel composition	correlation length, nm (DLS, 20 °C)
0.33 mol/L NIPAM, cross-linker 1:4320	8.0
0.33 mol/L NIPAM, cross-linker 1:2160	7.0
0.33 mol/L NIPAM, cross-linker 1:1080	7.0
0.33 mol/L NIPAM, cross-linker 1:540	6.0

Table 2. PNIPAM Hydrogel Gold Composite Samples: Composition and Correlation Length As Determined by DLS for Corresponding Pure Hydrogels without Added Gold Nanoparticles

Au nanoparticles, nm	hydrogel composition	correlation length, nm (DLS, 20 °C) (from pure hydrogels, see text)
20	0.33 mol/L NIPAM, cross-linker 1:330	7.5
50	0.33 mol/L NIPAM, cross-linker 1:330	7.5
100	0.33 mol/L NIPAM, cross-linker 1:330	7.5
100	0.50 mol/L NIPAM, cross-linker 1:700	9.0
100	0.33 mol/L NIPAM, cross-linker 1:700	10.0
100	0.20 mol/L NIPAM, cross-linker 1:700	121
100	0.15 mol/L NIPAM, cross-linker 1:700	"heterogeneous"
100	0.10 mol/L NIPAM, cross-linker 1:700	"heterogeneous"
100	0.33 mol/L NIPAM, cross-linker 1:1062	7.5
100	0.33 mol/L NIPAM, cross-linker 1:708	8.0
100	0.33 mol/L NIPAM, cross-linker 1:531	6.5
100	0.33 mol/L NIPAM, cross-linker 1:354	8.0
100	0.33 mol/L NIPAM, cross-linker 1:265	6.0

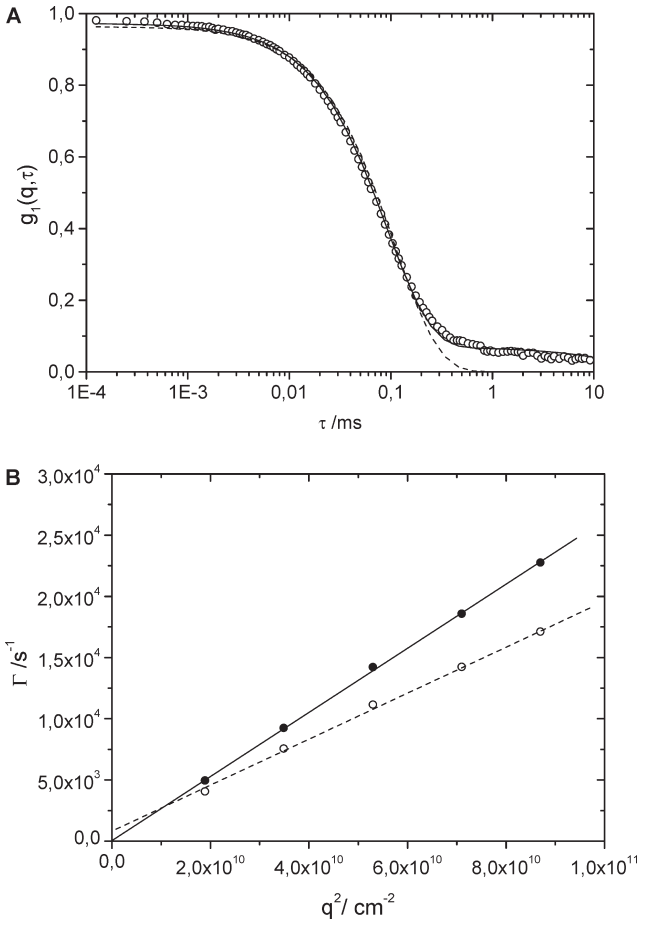

Figure 1. (A) DLS amplitude time-correlation function for pure hydrogel (polymer concentration 0.33 mol/L (= 4 vol %) NIPAM, cross-linker monomer ratio 1:531) (symbols) with single-exponential fit (dashed line) and double-exponential fit (solid line); T = 20 °C, scattering angle = 70°. (B) q^2-scaling of the relaxation rates determined for the dominant fast relaxation process by single-exponential fitting (dashed line) and by double-exponential fitting (solid line).

transparency or comparatively small average scattering intensity at room temperature. Only at polymer concentrations which are smaller than 0.20 mol/L, the hydrogel samples were more turbid and also showed strong indications of spatial and dynamical heterogeneities or nonergodicity, like an intercept much smaller than 1 in the correlations function and an average mesh size varying with sample position and/or scattering angle. For these gels, as also indicated in Table 2, it was not any longer possible to obtain reliable correlation functions and therefore to determine average mesh sizes by dynamic light scattering.

It is interesting to note that the mesh sizes listed in Table 2 depend strongly on polymer concentration but are nearly independent, within experimental error ±1.5 nm, of the degree of cross-linking. This is in agreement with the previous results by Shibayama et al.[8] and underlines the fact the correlation length extracted by dynamic light scattering from polymer gels is not a true mesh size, that is, a fixed hole pinned by chemical cross-links, but rather a highly dynamic structure defined by physical cross-links of polymer chains and therefore independent of cross-linker concentration but strongly dependent on polymer chain concentration and on homogeneity of the gel structure. Note, however, that the dependence of correlation length on polymer concentration shown in Table 2 is stronger than expected: actually, the correlation length seems to diverge at polymer concentrations that are smaller than 0.20 mol/L. For semidilute polymer solutions without cross-linker, one would expect a scaling of the correlation length with c 0.75, that is, for polymer concentrations 0.50, 0.33, and 0.20 mol/L 8, 11, and 16 nm instead of our experimental values 9, 10, and 121 nm (see Table 2). Although the first two numbers at polymer concentrations 0.50 and 0.33 agree within experimental error with theoretical expectation, as already stated in the Introduction, the presence of the cross-linker leads to a highly heterogeneous gel structure for polymer concentration 0.20 mol/L and smaller. This we also experimentally confirmed by an increase in scattering intensity, average correlation length, and indications of nonergodic behavior mentioned above.

To estimate the effect of chemical cross-links on tracer particle mobility, we also calculated the average size of a mesh, assuming for simplification a homogeneous distribution of cross-linker molecules on a simple cubic lattice and 100% conversion during the polymerization reaction. For cross-linker ratios between 1:540 and 1:4320 (see Table 1) we thereby obtained mesh sizes ranging from 14.0 to 27.9 nm. These meshes are much smaller than our gold probe particles of sizes 50 and 100 nm and in the range of our smallest 20 nm particles. Therefore, if our gel structure would indeed be perfectly homogeneous, we would expect no tracer mobility at room temperature in all cases. The fact that our probe particles of sizes 20 and 50 nm show a finite electrophoretic mobility within PNIPAM hydrogels at room temperature (see Figure 5) tells us that even well below the phase transition temperature the structure of PNIPAM hydrogels is heterogeneous, divided into highly cross-linked and less-cross-linked polymer chain solution-like domains. It remains to be seen how the phase transition opens up even larger path ways through the mesh structure leading to a strong enhancement in tracer mobility (see Figures 6 and 7).

Finally, we tried to extract the length scale of these structural heterogeneities from our double-exponential fitting: this length scale was increasing from several hundred nanometers to several ten thousand nanometers with decreasing polymer concentration at fixed cross-linker concentration but also with decreasing cross-linker concentration at fixed polymer concentration. Note, however, that these values could not be determined very accurately due to the small amplitude of the slow relaxation process as well due to insufficient accumulation time for such slow modes.

Let us discuss the effect of sample temperature on the gel structure. Figure 2 shows the correlation functions, measured for a pure hydrogel, with NIPAM concentration 0.33 mol/L and cross-linker:monomer ratio 1:540, at various temperatures. From T = 20 °C to T = 24 °C, the correlation length of the dominant fast process is slightly increasing, but as judged from the signal intercept and the nearly single-exponential decay, the system remains fairly homogeneous. At T = 28 °C, the slow mode representing spatial heterogeneities gains in amplitude, and the correlation length defined by the fast mode is starting to diverge. Finally, at T = 33 °C, the intercept is much lower than 1.0, and the slow relaxation process is much more pronounced, both indications of increasing dynamical heterogeneities (nonergodic behavior). These results agree very well with the previous neutron scattering studies of Shibayama et al.[22]

Next, we consider the variation in mesh size (or, better, correlation length of the dominant fast relaxation process) with temperature as quantified by double-exponential fitting of the dynamic light scattering correlation functions displayed in Figure 2. As shown in Figure 3, and also already described by Shibayama et al.,[22] this mesh size increases with

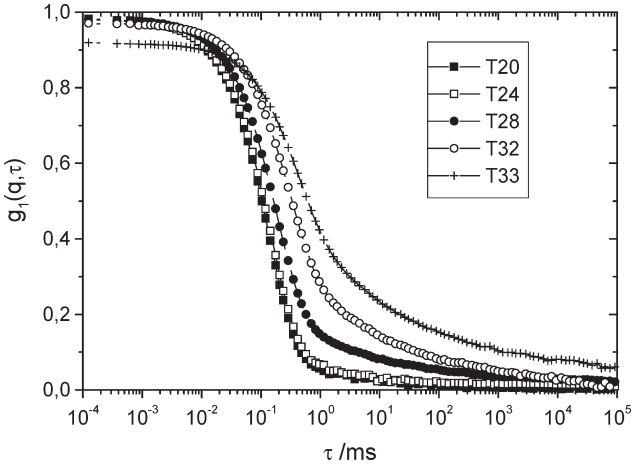

Figure 2. Amplitude−time-correlation functions for PNIPAM hydrogel (polymer concentration 0.33 mol/L NIPAM, degree of cross-linking 1:540), scattering angle 50°, measured at $T = 20$ °C to $T = 33$ °C. Lines are guides to the eye only.

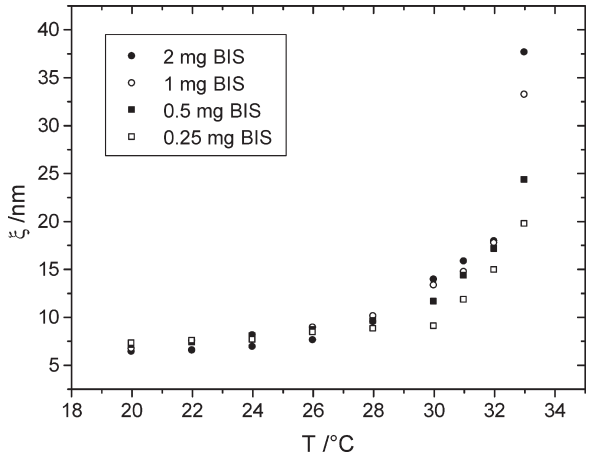

Figure 3. Average correlation lengths extracted from DLS correlation functions (all measured at scattering angle 50°) versus sample temperature for various PNIPAM hydrogels (polymer concentration 0.33 mol/L NIPAM, degree of cross-linking 1:4320 (open squares), 1:2160 (solid squares), 1:1080 (open circles), and 1:540 (solid circles)).

temperature and finally diverges close to the transition temperature $T = 34$ °C. Importantly, the increase is the more pronounced the higher the cross-link density. Although dynamic light scattering of gels is commonly known as a nontrivial task due to the problem of nonergodicity, our results agree remarkably well with the previous finds of Shibayama et al.: on the basis of our own dynamic light scattering measurements and the results presented in ref 22, we conclude that with increasing sample temperature the PNIPAM hydrogel becomes more and more heterogeneous, and therefore the length scale of a bicontinuous structure of solution-like domains in between tightly cross-linked solid-like domains increases. As a consequence with respect to our added gold tracers, we expect that this increase in effective pore size should also lead to an increase in electrophoretic mobility of the gold nanoparticles as well. Importantly, the correlation length shown in Figure 3 does not seem to correspond to this effective pore size, but rather is the correlation length within the solution-like domains: with increasing temperature, not only the overall length scale but also the polymer concentration within these domains seem to decrease. In the next section, we will demonstrate how the mobility of nanoscopic probe particles is utilized

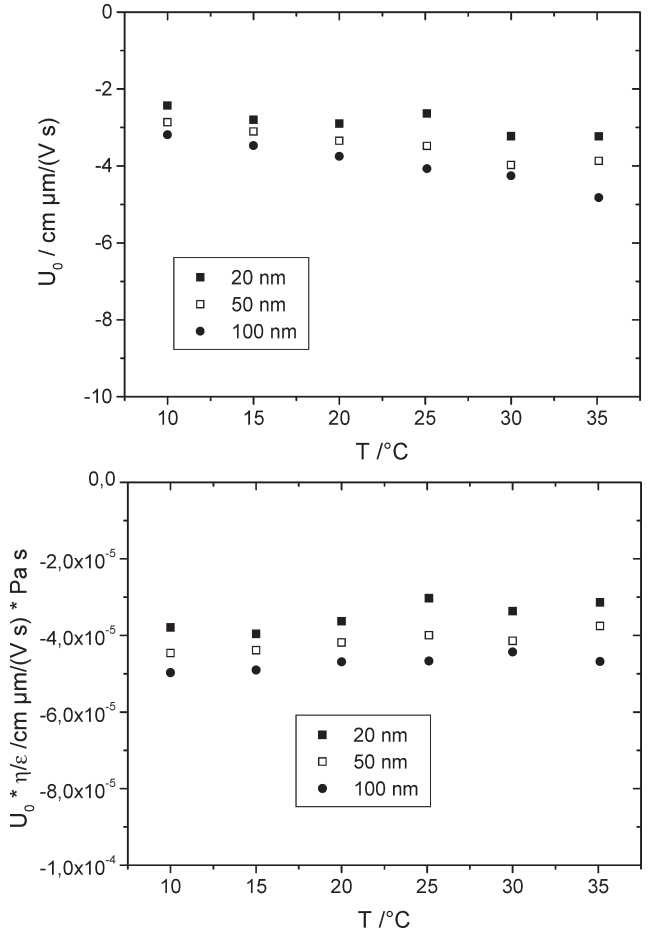

Figure 4. Electrophoretic mobility of gold nanoparticles of sizes 20, 50, and 100 nm in pure water (U_0) as a function of sample temperature (top) and the same data normalized by solvent viscosity and dielectric constant (bottom).

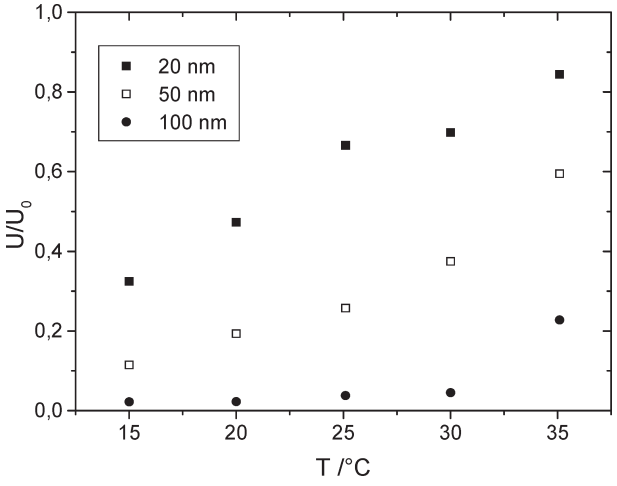

Figure 5. Electrophoretic mobility of gold nanoparticles of sizes 20, 50, and 100 nm in a PNIPAM hydrogel (polymer concentration 0.33 mol/L NIPAM, cross-linker ratio 1:330) as a function of sample temperature, normalized by the mobility in pure water U_0.

to explore our heterogeneous hydrogel structure in more detail.

2. Electrophoretic Mobility of Gold Nanoparticles. *Pure Water*. In Figure 4, we show the electrophoretic mobilities of gold nanoparticles of different sizes in pure water measured by phase analysis light scattering as a function of sample

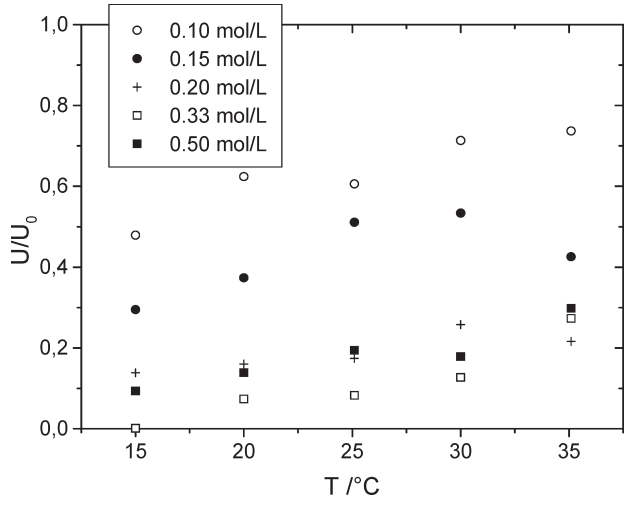

Figure 6. Electrophoretic mobility of gold nanoparticles of size 100 nm in PNIPAM hydrogels (polymer concentration ranging from 0.10 to 0.50 mol/L NIPAM, cross-linker ratio 1:700) as a function of sample temperature, normalized by the mobility in pure water U_0.

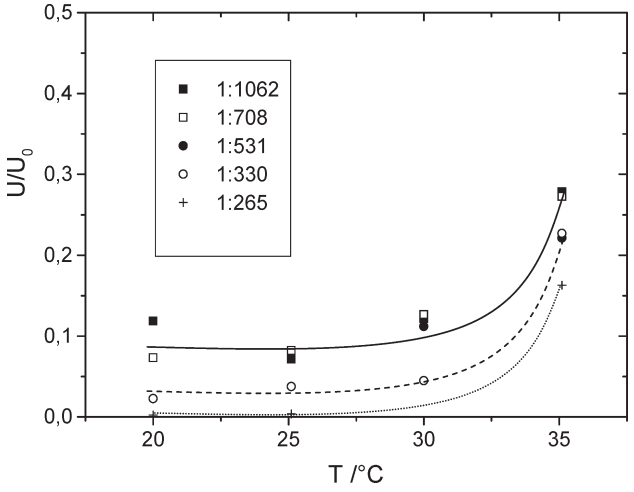

Figure 7. Electrophoretic mobility of gold nanoparticles of size 100 nm in PNIPAM hydrogels (polymer concentration 0.33 mol/L NIPAM, cross-linker ratio from 1:1062 to 1:265) as a function of sample temperature, normalized by the mobility in pure water U_0. Lines are guides to the eye.

temperature. This mobility depends not only on particle size and particle charge but also on the temperature-dependent solvent properties viscosity and dielectric constant. To separate these effects, we normalized our data accordingly (see Figure 4, bottom). As expected, these normalized mobilities are independent of sample temperature and slightly dependent on particle size. Larger particles have the higher mobility due to their higher surface charge, which increases with the particle size squared, whereas the hydrodynamic friction only increases linearly with particle size (see also eq 2).

However, the corresponding effect of particle size on electrophoretic mobility is smaller than expected for a constant surface charge density, indicating that for our three gold probes the charge density is decreasing with increasing particle size, an effect probably based on surface curvature: smaller particles have a higher surface curvature and therefore a higher area concentration of bulky ligand molecules bound to the nanoparticle surface.

In the following, we use the mobilities shown in Figure 4 (top) as reference values to normalize the mobilities measured for the gold tracers in various hydrogels. In this way, the effects of temperature on solvent viscosity and dielectric constant are eliminated, and the resulting reduced particle mobility should depend on the influence of sample temperature on the mesh structure of the PNIPAM hydrogels only.

PNIPAM Hydrogel: Effect of Particle Size and Sample Temperature. Figure 5 shows the normalized mobilities of gold tracers of three different sizes embedded in identical hydrogels of polymer concentration 0.33 mol/L and cross-link density 1:330 as a function of sample temperature.

As expected, at given sample temperature the mobility is the higher the smaller the tracer particles and in all cases smaller than the mobility in pure water. With increasing temperature, the mobility is also increasing, but in contrast to the mesh sizes shown in Figure 3, which are diverging at $T > 34$ °C, the mobility increases almost linearly with temperature for the two smaller gold tracers. Those particles show at least 10% of their mobility in pure water already at room temperature, so the effective mesh size of the hydrogel in respect to the gold particle size has to be comparatively large, definitely much larger than the theoretically expected value for a perfectly homogeneous gel of 11.8 nm (assuming a simple cubic lattice as described before). This tells us, as mentioned before, that the mesh sizes or correlation lengths given in Tables 1 and 2 and shown in Figure 3 are not to be taken literally as the diameters of fixed pores within the hydrogel; otherwise, gold nanoparticles of sizes 20 and 50 nm should be completely trapped and show zero mobility. Also, the theoretically expected mesh size of 11.8 nm does not fit to our probe particle mobilities. Rather, as deduced from the finite mobility of our medium tracers of size 50 nm (= about 20% of the mobility in pure water; see Figure 5) and the near-complete immobilization of our largest tracers of size 100 nm, even at room temperature we expect permanently fixed meshes much larger than 50 nm but smaller than 100 nm. This result that the mesh size between chemical cross-links has to be much larger than theoretically expected tells us that either the conversion rate of the cross-linker is much smaller than 100% or the cross-linker is not distributed homogeneously but the sample consists of tightly cross-linked solid-like domains and more liquid-like domains, a structure of PNIPAM hydrogels already described by Shibayama and co-workers.[8,12,22,26,27] Here, the liquid-like domains may constitute a path for the migration of the gold particles. This structural heterogeneity is very plausible considering the difference in chemical reactivity of cross-linker and NIPAM monomer and also taking into account that our DLS correlation functions even at room temperature showed a bimodal decay (see Figure 1). Within the liquid-like domains, the correlation length corresponds to the value expected (and measured) for corresponding non-cross-linked homogeneous polymer solutions. These correlation lengths of less than 10 nm measured independently by DLS and SANS are not a fixed obstacle to tracer particle migration but rather highly flexible physical interchain contacts, and our gold nanoparticles can squeeze through these fluctuating meshes even though their diameter is much larger than this correlation length.

As mentioned, for our largest tracer particles of size 100 nm, the mobility at room temperature is very small compared to that found in pure water (<2%, see Figure 5). These particles obviously are too large to squeeze through the pores at low temperature, that is, through the path created by the solution-like domains. With increasing temperature approaching the phase transition, when the sample becomes more and more heterogeneous and therefore the characteristic length scale of the solution-like domains becomes much

larger than 100 nm, the mobility of the 100 nm tracers increases considerably, reaching more than 20% of that found in pure water. Here, mesh size and tracer mobility follow a similar trend of divergence at the phase transition. Note that according to this argument the length scale of the solution-like domains has to be much larger than the length scale of the mesh size determined by DLS (see Figure 3). Our assumption is that the highly cross-linked domains collapse at the phase transition, leading to an increase in length scale of the non-cross-linked domains as well as a decrease in their polymer concentration. Therefore, the correlation length probed by dynamic light scattering, which is depending on polymer concentration, is also increasing with increasing sample temperature.

On the other hand, as mentioned, the smallest tracers of size 20 nm show an almost linear increase in mobility with increasing temperature and the medium tracers of size 50 nm only a slight indication of divergence. Here, it has to be taken into account that the smallest tracers in the hydrogel at room temperature already have a mobility of more than 40% of that found in pure water. Since the maximum possible value is the pure water mobility, the tracer mobility therefore can only increase by a factor of 2, providing not much room for divergence. Simply stated, these tracers are so small that even the small length scale of polymer solution-like domains found at room temperature does not provide much of an obstacle to the tracer movement. Therefore, even if this length scale is strongly increasing or seems to diverge at the phase transition, the resultant effect on tracer mobility has to be much less pronounced. The situation is different for tracer particles being similar in size to the length scale of the polymer solution-like domains at room temperature: whereas these particles should be nearly immobilized at room temperature, the considerable increase in length scale of the liquid-like domains with increasing temperature leads to a corresponding gain in tracer mobility.

The data shown in Figure 5 not only enhance our understanding of the meaning of the correlation length as a "dynamic mesh size" but also nicely illustrate how the change in gel structure with increasing temperature is probed by the mobility of added nanoscopic tracers. Note that even for our hydrogel with highest cross-link density 1:330 and polymer concentration 0.33 mol/L, where the correlation length or dynamic mesh size probed by dynamic light scattering is smaller than 10 nm, the length scale of the polymer solution-like domains has to be larger than 50 nm or, as formulated by Shibayama et al., the gelation threshold is not yet reached.[8] They report a value of 1:160 at polymer concentration 0.2 mol/L to encounter zero mobility of their 85 nm tracers, claiming that "the most important factor to rule probe diffusion is whether the system has a permanent infinite network" structure. Our data show, however, that the size of the probe particles is also important, so not only the permanent network structure but also its inherent length scale, that is, the size of "pores" of non-cross-linked solution-like domains in between the chemically cross-linked solid-like domains, plays an important role. Even if the network is permanent, it still may be interpenetrated by a continuous solution-like phase with length scale large enough to guarantee some probe particle mobility.

PNIPAM Hydrogel: Effect of Polymer Concentration and Sample Temperature. Figure 6 shows the normalized electrophoretic mobilities of our large 100 nm gold tracers in hydrogels with identical cross-link density 1:700 but different polymer concentrations. Note that the tracer mobility shown in Figure 6 (cross-linker 1:700) at given temperature is much larger than that in Figure 5 (cross-linker 1:330), so the degree of cross-linking as expected has a strong influence on the tracer mobility and therefore on the dynamics of the meshes, although not much effect on the correlation length determined by DLS for pure hydrogels itself (see Tables 1 and 2). Surprisingly, at the highest three polymer concentrations 0.20, 0.33, and 0.50 mol/L NIPAM, which also show nearly identical correlation lengths, the polymer content of the hydrogel seems to have no detectable systematic effect on the tracer mobility. There is a nearly constant and similar increase in tracer mobility with temperature from about 10% (at $T = 20$ °C) to about 25% (at $T = 35$ °C) of that found in pure water, that is, a relative increase in mobility by more than 100%, for all three samples. At smaller polymer concentrations, where hydrogels also according to dynamic light scattering have much larger mesh sizes and finally become heterogeneous (see Table 2), the gold tracer mobility is higher than 30% of that in pure water but only shows a relatively moderate increase by about 50% with sample temperature (from 30% to 50% for $c = 0.15$ mol/L and from 50% to 70% for $c = 0.10$ mol/L). In case of such low polymer concentrations, < 0.20 mol/L NIPAM, the gel is already quite heterogeneous at room temperature, leading already to an enhanced tracer particle mobility so the phase transition only has a minor effect.

PNIPAM Hydrogel: Effect of Degree of Cross-Linking and Sample Temperature. Finally, we explored the effect of cross-linking density on temperature-dependent tracer mobility at given polymer concentration 0.33 mol/L in more detail, as shown in Figure 7. For the hydrogel with the highest cross-link density 1:265 the tracer mobility is nearly zero at small sample temperature and increases to about 15% of the mobility found in pure water at the transition temperature. The samples with the lowest cross-link densities 1:531, 1:708, and 1:1062 all show similar tracer mobilities within experimental error. At room temperature, these three hydrogels possess the highest tracer mobility (about 10% of the pure water value) of all samples shown in Figure 7, increasing to almost 30% at the phase transition. The sample with cross-link content 1:330 shows an intermediate behavior, as expected. Our data lead to the conclusion that at low temperature, although according to dynamic light scattering all samples have comparable correlation lengths (see Table 2), the effective pores or solution-like domains become smaller with increasing cross-linker content, and therefore the tracer mobility becomes smaller. At cross-linker ratio $< 1:300$, the mobility of our 100 nm gold tracers finally becomes zero at room temperature within experimental resolution. On the other hand, the phase transition dramatically changes the mesh structure of the hydrogel, leading to an increase in effective pore size or length scale of polymer solution-like domains which is more pronounced the higher the cross-linker concentration (see also ref 22). Consequently, the tracer mobility is increasing with the relative increase in probe particle mobility with increasing temperature; also, the more pronounced, the higher the cross-link density, as seen in Figure 7.

Conclusions

We studied the electrophoretic mobility of gold nanoparticles in thermoresponsive poly(*N*-isopropylacrylamide) (PNIPAM) hydrogels by phase analysis dynamic light scattering (PALS) in dependence of sample temperature, size of the gold nanoparticles, and structure of the hydrogel (polymer content and cross-linker content). The fact that comparatively large tracers move through comparatively smaller meshes (or, better, correlation lengths) allows conclusions on the dynamic nature of these gel meshes as

well as on the bicontinuous structure consisting of chemically cross-linked solid-like domains and polymer solution-like domains, the latter providing the path for probe particle migration. Approaching the phase transition temperature, the mobility of the probes strongly increased in all cases, which is related to the spinodal decomposition of the gel into polymer-poor and highly cross-linked polymer-rich domains, opening up even larger pores which allow for enhanced migration of the embedded particles. The degree of cross-linking and the polymer concentration have an effect both on tracer mobility at room temperature and on the degree in structural change at the phase transition. The latter was explored in some detail by temperature-dependent electrophoretic mobility measurements of added gold nanotracers. These experiments proved to be an efficient and technically simple tool to explore the mesh structure of polymer gels, compared to more complicated and time-consuming neutron scattering measurements. Also, they are easier than dynamic light scattering measurements, since only the mobility of the tracers is detected, and therefore the nonergodicity of the gel matrix, or the separation of different relaxation processes, does not provide any problems. Detailed information on the heterogeneous structure of the gels as a function of temperature can be obtained by systematic variation of the size of the tracers, which provides a direct measure for the dominant length scale of polymer-poor domains within the gel.

Using nonisotropic nanotracers, as for example gold nanorods,[28−30] and probing their rotational relaxation directly by polarized video microscopy may further enhance the possibilities of this scheme in the future. Finally, investigating the temperature-enhanced dynamics of nanoscopic probes within a thermoresponsive hydrogel matrix is also interesting with respect to thermally controlled release of nanoscopic substrates from thermoresponsive hydrogels for biomedical applications.

References and Notes

(1) Park, I. H.; Johnson, C. S. *Macromolecules* **1990**, *23*, 1548.
(2) Suzuki, Y.; Nishio, I. *Phys. Rev. B* **1992**, *45*, 4614.
(3) Bu, Z.; Russo, P. S. *Macromolecules* **1994**, *27*, 1187.
(4) Pajevic, S.; Bansil, R.; Konak, C. *Macromolecules* **1995**, *28*, 7536.
(5) Tokita, M.; Miyoshi, T.; Takegoshi, K.; Hikichi, K. *Phys. Rev. E* **1996**, *53*, 1823.
(6) Matsukawa, K.; Yasunaga, H.; Zhao, C.; Kuroki, S.; Kurosu, H.; Ando, I. *Prog. Polym. Sci.* **1999**, *24*, 995.
(7) Waigh, T. A. *Rep. Prog. Phys.* **2005**, *68*, 685.
(8) Shibayama, M.; Isaka, Y.; Shiwa, Y. *Macromolecules* **1999**, *32*, 7086–7092.
(9) Mallam, S.; Horkay, F.; Hecht, A.-M.; Geissler, E. *Macromolecules* **1989**, *22*, 3356.
(10) Schild, H. G. *Prog. Polym. Sci.* **1992**, *17*, 163.
(11) Matsuo, E. S.; Orkisz, M.; Sun, S.-T.; Li, Y.; Tanaka, T. *Macromolecules* **1994**, *27*, 6791.
(12) Shibayama, M.; Norisuye, T.; Nomura, S. *Macromolecules* **1996**, *29*, 8746.
(13) Pusey, P. N.; van Megen, W. *Physica A* **1989**, *157*, 705.
(14) Pusey, P. N.; van Megen, W.; Underwood, S. M.; Bartlett, P.; Ottewill, R. H. *J. Phys.: Condens. Matter* **1990**, *2*, SA373–SA377.
(15) Stanton, S. G.; Pecora, R.; Hudson, B. S. *J. Chem. Phys.* **1981**, *75*, 5615.
(16) Schartl, W.; Roos, C. *Phys. Rev. E* **1999**, *60*, 2020.
(17) Spill, R.; Köhler, W.; Lindenblatt, G.; Schaertl, W. *Phys. Rev. E* **2000**, *62*, 8361.
(18) Sershen, S. R.; Westcott, S. L.; Halas, N. J.; West, J. L. *J. Biomed. Mater. Res.* **2000**, *51*, 293–298.
(19) Sershen, S. R.; Westcott, S. L.; West, J. L.; Halas, N. J. *Appl. Phys. B* **2001**, *73*, 379–381.
(20) Sershen, S. R.; Westcott, S. L.; Halas, N. J.; West, J. L. *Appl. Phys. Lett.* **2002**, *80*, 4609–4611.
(21) Shiotani, A.; Mori, T.; Niidome, T.; Niidome, Y.; Katayama, Y. *Langmuir* **2007**, *23*, 4012–4018.
(22) Shibayama, M.; Tanaka, T.; Han, C. C. *J. Chem. Phys.* **1992**, *97*, 6829–6841.
(23) Tokita, M.; Tanaka, T. *Science* **1991**, *253*, 1121–1123.
(24) Ohshima, H. *J. Colloid Interface Sci.* **2001**, *239*, 587–590.
(25) Tscharnuter, W. W. *Appl. Opt.* **2001**, *40*, 3995–4003.
(26) Shibayama, M.; Tanaka, T. *Adv. Polym. Sci.* **1993**, *109*, 1–62.
(27) Shibayama, M. *Macromol. Chem. Phys.* **1998**, *199*, 1.
(28) Murphy, C. J.; San, T. K.; Gole, A. M.; Orendorff, C. J.; Gao, J. X.; Gou, L.; Hunyadi, S. E.; Li, T. *J. Phys. Chem. B* **2005**, *109*, 13857–13870.
(29) Link, S.; El-Sayed, M. A. *J. Phys. Chem. B* **1999**, *103*, 8410–8426.
(30) Yu, Y. Y.; Chang, S. S.; Lee, C. L.; Wang, C. R. C. *J. Phys. Chem. B* **1997**, *101*, 6661–6664.